sustainability

MDPI

Article

Carbon Nanotube/Pt Cathode Nanocomposite Electrode in Microbial Fuel Cells for Wastewater Treatment and Bioenergy Production

Mostafa Ghasemi [1,*], Mehdi Sedighi [2] and Yie Hua Tan [3]

[1] Chemical Engineering Section, Faculty of Engineering, Sohar University, Sohar 311, Oman
[2] Department of Chemical Engineering, University of Qom, Qom 3716146611, Iran; sedighi@qom.ac.ir
[3] Department of Environmental Engineering, Faculty of Engineering and Science, Curtin University, Miri 98009, Sarawak, Malaysia; tanyiehua@curtin.edu.my
* Correspondence: MBaboli@su.edu.om

Abstract: In this paper, we reported the fabrication, characterization, and application of carbon nanotube (CNT)-platinum nanocomposite as a novel generation of cathode catalyst in microbial fuel cells (MFCs) for sustainable energy production and wastewater treatment. The efficiency of the carbon nanocomposites was compared by platinum (Pt), which is the most effective and common cathode catalyst. This nanocomposite is utilized to benefit from the catalytic properties of CNTs and reduce the amount of required Pt, as it is an expensive catalyst. The CNT/Pt nanocomposites were synthesized via a chemical reduction technique and the electrodes were characterized by field emission scanning electron microscopy, electronic dispersive X-Ray analysis, and transmission electron microscopy. The nanocomposites were applied as cathode catalysts in the MFC to obtain polarization curve and coulombic efficiency (CE) results. The catalytic properties of electrodes were tested by linear sweep voltammetry. The CNT/Pt at the concentration of 0.3 mg/cm^2 had the highest performance in terms of CE (47.16%), internal resistance (551 Ω), COD removal (88.9%), and power generation (143 mW/m^2). In contrast, for the electrode with 0.5 mg/L of Pt catalyst, CE, internal resistance, COD removal, and power generation were 19%, 810 Ω, 96%, and 84.1 mW/m^2, respectively. So, it has been found that carbon nanocomposite cathode electrodes had better performance for sustainable clean energy production and COD removal by MFC.

Keywords: carbon nanotube; coulombic efficiency; microbial fuel cell; nanocomposite; Pt

Citation: Ghasemi, M.; Sedighi, M.; Tan, Y.H. Carbon Nanotube/Pt Cathode Nanocomposite Electrode in Microbial Fuel Cells for Wastewater Treatment and Bioenergy Production. *Sustainability* **2021**, *13*, 8057. https://doi.org/10.3390/su13148057

Academic Editor: Farooq Sher

Received: 13 June 2021
Accepted: 17 July 2021
Published: 19 July 2021

1. Introduction

Climate change and the risk of running out of non-renewable energy has made scientists think about clean alternative types of fuels [1–3]. In addition, as a consequence of population growth and the industrial revolution, the energy demand has been on an upward trend, and also a large volume of wastewater is produced [4,5]. Therefore, there is a considerable request globally for reliable, clean energy sources and wastewater treatment plants. The microbial fuel cells (MFC) are an apparatus that converts the chemical energy of biodegradable organic compounds to electricity and hydrogen, which are the clean and renewable types of energy [6,7]. This means that an MFC can utilize the organic compound of waste and produce energy, thus, treating wastewater [8–11] and producing energy simultaneously [7]. Generally, MFCs consist of two chambers, namely cathode, and anode divided by a separator or proton exchange membrane (PEM) [12,13]. The anode chamber utilizes organic matter to produce electrons, which are transferred to the cathode chamber via an external circuit. The produced protons will pass through the separator to reach the cathode chamber. Lots of efforts have been made to make the MFCs commercial [14,15]. Most of the expenses of an MFC are due to its cathode catalyst (Pt), which accelerates the oxygen reduction reaction (ORR). According to the

reports, more than half of MFC price is related to Pt [16,17]. Platinum is a durable and efficient catalyst, which is adopted for MFC and makes the ORR faster. However, it is very expensive and is not applicable for use on a large scale. Therefore, researchers tried to find a catalyst other than Pt or decrease the amount of Pt in the MFC. Among all the materials, carbon nano-based materials and nanocomposites attracted lots of attention due to their unique properties. They possess a substantial specific surface area with high catalytic activity and showed promising properties in electron production and transfer [18–20]. Jafar Ali et al. [21] used nanocomposite iron sulfide wrapped with graphene oxide as the cathode catalyst. The MFC with nanocomposite cathode catalyst presented a higher removal of toxic Cr and a 4.6 higher reduction rate than blank MFC [22]. Moreover, the MFC which used nanocomposite cathode catalyst produced 3.28 times more power density. Another group of researchers [23] tried to replace the expensive cathode catalyst. They used two different multiwall carbon nanotube (CNT)-based cathode catalysts. These authors found that Co-N-CNT and Fe-N-CNT had higher ORR activity and also generated more power density than Pt [24]. In another, Pattanayak et al. [22] utilized poly (aniline co pyrrole) wrapped titanium dioxide nanocomposite for an air cathode MFC. They found that the nanocomposite catalyst produced 2.3 times higher power output than the Pt/c catalyst. In another interesting study, Yu Du et al. [25] replaced Pt as an expensive cathode catalyst with a hybrid nanocomposite catalyst. They used nitrogen-doped CNT, reduced graphene oxide nanosheet, and compared this new catalyst with Pt. These researchers could produce 1329 mW/cm^2 power density which was 1.37 times higher than Pt catalyst.

In a recent investigation, Yan Wang et al. [26] synthesized a bimetallic hybrid modified with CNT and applied it as a cathode catalyst in MFC. The newly synthesized cathode catalyst had higher ORR performance and produced 2757 mW/m^3 power density which was higher than Pt (2313 mW/m^3) catalyst.

In 2019, Majidi et al. fabricated α-MnO_2/C, and α-MnO_2/C supported on carbon Vulcan catalyst for air cathode MFC. The catalysts could produce 180 and 111 mW/m^2, respectively. However, the produced powers were not that much higher, but the catalysts were considered as economical compared to the pure Pt catalyst [27].

Sofia et al. have done a study on platinum group metal-free based catalyst in 2020. However, they reported that the power output is increased but the generated power was 67.3 mW/m^2 and 120 mW m^{-2} after 35 days and two months respectively. The power densities were quite low and also the power output changed a lot due to the fluctuating environmental condition [28].

As different parameters influence the performance of MFC, Ghasemi et al. [24] used two methods for optimizing MFC. They tried artificial intelligence and fuzzy logic. The mentioned authors considered diverse optimized conditions and interestingly observed that each optimization technique produced a certain result.

However, there are lots of studies about synthesis and applications of new catalysts in MFCs, there are not many studies about optimization of Pt and making MFCs more economical by Pt composite catalysts. As the Pt is the most efficient and durable catalyst and also the most expensive, we tried to reduce the amount of Pt, but not eliminate it.

This research is a big step towards the commercialization of MFC because it use a smaller amount of Pt as the cathode catalyst, thus making MFC a sustainable method for use on a bigger scale for societies and industries. Until now, MFC has not been applied widely as it is not a sustainable solution for wastewater treatment and energy production. However, the scientists had lots of progress in improving the MFCs for higher power generation and wastewater treatment [4].

In the present study, CNT/Pt nanocomposite has been synthesized and characterized. Furthermore, the optimum amount of this catalyst was found for using in MFC to reach higher ORR potential, COD removal, and power generation. The self-generated nanocomposite was made and applied as a cathode catalyst in MFC and the performance of this option was compared with Pt catalyst.

2. Materials and Methods

2.1. MFC Configuration

The design of MFC was the same as in previous studies [29]. It consisted of two cylindrical chambers with a length of 14 cm and a diameter of 6.2 cm (300 cm^3 active volume) separated by Nafion 117 (China). The membrane was pretreated before use by boiling water and 3% hydrogen peroxide, or 0.5 M sulfuric acid for half an hour and kept inside deionized water. The cathode and anode electrodes had 12 cm^2 surface area [29]. The 0.5 M phosphate buffer solution was used to adjust the pH of the solution around 6.5–7. The cathode chamber consisted of 4.26 g/L Na_2PO_4, 2.5 g/L NaH_2PO_4, 0.13 g/L KCl, and 0.31 g/L NH_4Cl solution, and aeration was performed by an aquarium pump. Carbon paper (CP) was utilized as the anode electrode, in addition to Pt and CNT/Pt being employed at different concentrations as the cathode electrode. Figure 1 shows the schematic of an MFC. The protons passed through PEM and electrons were transferred through the external circuit to reach the cathode.

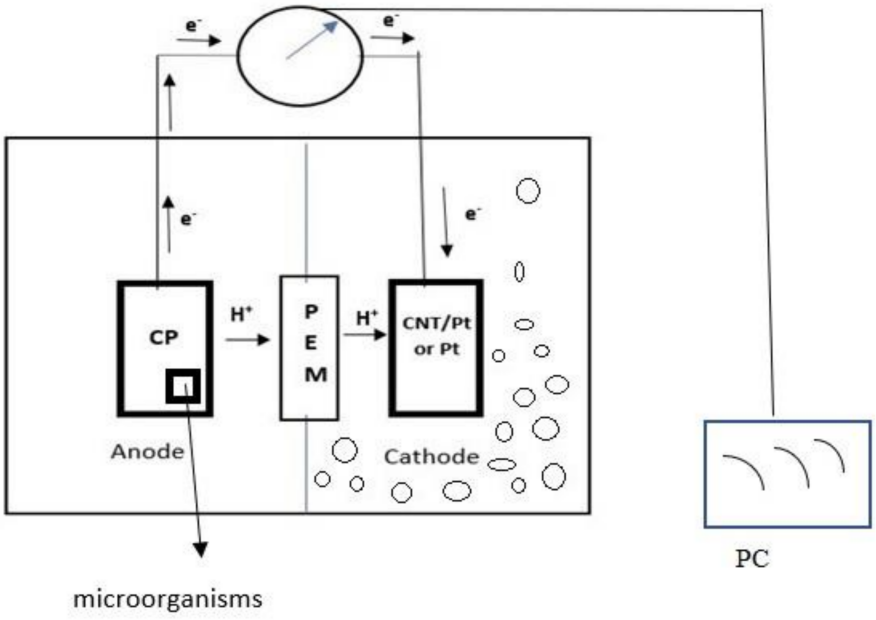

Figure 1. Schematic representation of the fabricated MFC.

For inoculation of MFC at the anode chamber, anaerobic sludge from a palm oil mill effluent treatment plant (Selangor, Malaysia) was utilized. The media comprised of 5 g glucose as the source of sugar, 0.5 g yeast extract, 4 g $NaHCO_3$, 0.2 g KCl, and 10 mL Wolfe's mineral and vitamin solution added per liter [30]. All the chemicals were provided by Merck Company (Darmstadt, Germany).

2.2. Electrode Preparation

2.2.1. Pt Electrode

For preparing Pt electrode, first, the Pt was washed with deionized water followed by filtering and drying in the oven. Next, Pt was dispersed in a Nafion solution resulting in Pt ink. The ink was dispersed on the CP electrode by a brush and was dried for 1 h at 100 °C in an oven [12].

2.2.2. CNT/Pt Nanocomposite Electrode

To produce CNT/Pt, the chemical reduction technique was used. In the first step, CNT was dispersed by ultrasonication in HNO_3 for 3 h. Afterward, the produced solution was dried, rinsed, and finally dried in the air. The resultant CNT sample was then dispersed by ultrasonication in $(CH_3)_2CO$ for 1 h. Next, the 0.075 molar H_2PtCl_6 solution was slowly

added to CNT during stirring. After 24 h, the mixture was reduced by 0.1 M $NaBH_4$ as well as 1 M NaOH solution. As soon as the mixture was uniformly mixed, it was rinsed and dried at 80 °C for almost 6 h [16]. The required quantity of CNT/Pt was added to a limited proportion of C_2H_5OH, dispersed properly on a mixer, and brushed on the CP surface. Afterward, the CNT/Pt electrode was placed in the oven at 100 °C to dry.

2.3. Analysis and Calculation

The experiments were done in three months and the data were collected in three days (72 h) when the system became stable.

Formulas (1) and (2) were utilized to determine the current as well as power density:

$$I = \frac{V}{R} \tag{1}$$

$$P = R \times I^2 \tag{2}$$

where I denotes the current (amps), R is the external resistance (ohm), V refers to the voltage (V), and P represents the produced power (Watt) of the system [31,32]. The coulombic efficiency (CE) was calculated as the actual current transferred to the maximum current that is obtainable from the system. It can be calculated by the following equation [18]:

$$CE = \frac{M \int_0^t I \, dt}{F \, b \, V_{an} \, \Delta COD} \tag{3}$$

where M refers to the molecular weight of oxygen (32 g/mole), F denotes the Faraday's constant (96,485 C/mol-electrons), $b = 4$ is the number of electron exchange per mole of oxygen, ΔCOD represents the change of COD over time t, and V_{an} is the liquid volume (m^3) in the anode chamber.

For measurement of the COD, first, the samples of media were diluted 10 times and then 2 mL of the dilute was mixed uniformly with (a vial) of high-range COD reagent digestion solution. Then it was heated to 150 °C by a thermo reactor (Hach, DRB 200, Loveland, CO, USA) for 2 h, and read with a spectrophotometer (Hach, DR 2800, Loveland, CO, USA) [33].

The experiments were performed three times under the same conditions and the mean values or typical results are presented below.

2.4. Electrodes Morphology and Catalytic Activity

The morphology of the surface of the electrodes and the attached bacterial community on the anode electrode was observed by field emission scanning electronic microscopy (FESEM) (Supra 55vp-Zeiss, Oberkochen, Germany). Before the FESEM analysis, the samples were entirely coated by a thin conducting metal, such as gold. Transmission electronic microscopy (TEM) (CM-12, Philips, Eindhoven, The Netherlands) was employed to find out the dispersion of Pt nanoparticles. The Energy-Dispersive X-ray spectroscopy (EDX) (INCA, Oxford, UK) was applied to detect the percentage of Pt in the nanocomposite. The catalytic activity of the electrodes was tested by a potentiostat galvanostat (HAK-MILIK FRIM 04699A-2007, Japan) in 0.1 M H_2SO_4 with the reference electrode of Ag/AgCl, working electrode of glassy carbon and Pt as counter electrode for linear sweep voltammetry (LSV) and 50 mV/S scan rate in the range of −1 until 0.4 V [34].

3. Results and Discussion

3.1. Electrode Characterization

Figure 2a,b show the FESEM, as well as TEM images of Pt-dispersed CNTs. The uniform dispersion of Pt nanoparticles in the CNTs can be observed in the TEM image, where the dark spots indicate the presence of Pt. The functionalization of CNTs using HNO_3 increased the surface reactivity and active sites of CNTs facilitating the fine dispersion of Pt nanoparticles on the CNT surface [35]. It enhances electrode electrochemical activity

due to the high catalytic surface area of CNT and the supportive and catalytic effects of Pt [36]. The EDX pattern shown in Figure 2c indicates the percentage of CNT and Pt in the nanocomposite. The Pt weight percentage to CNT ratio was found to be around 25%.

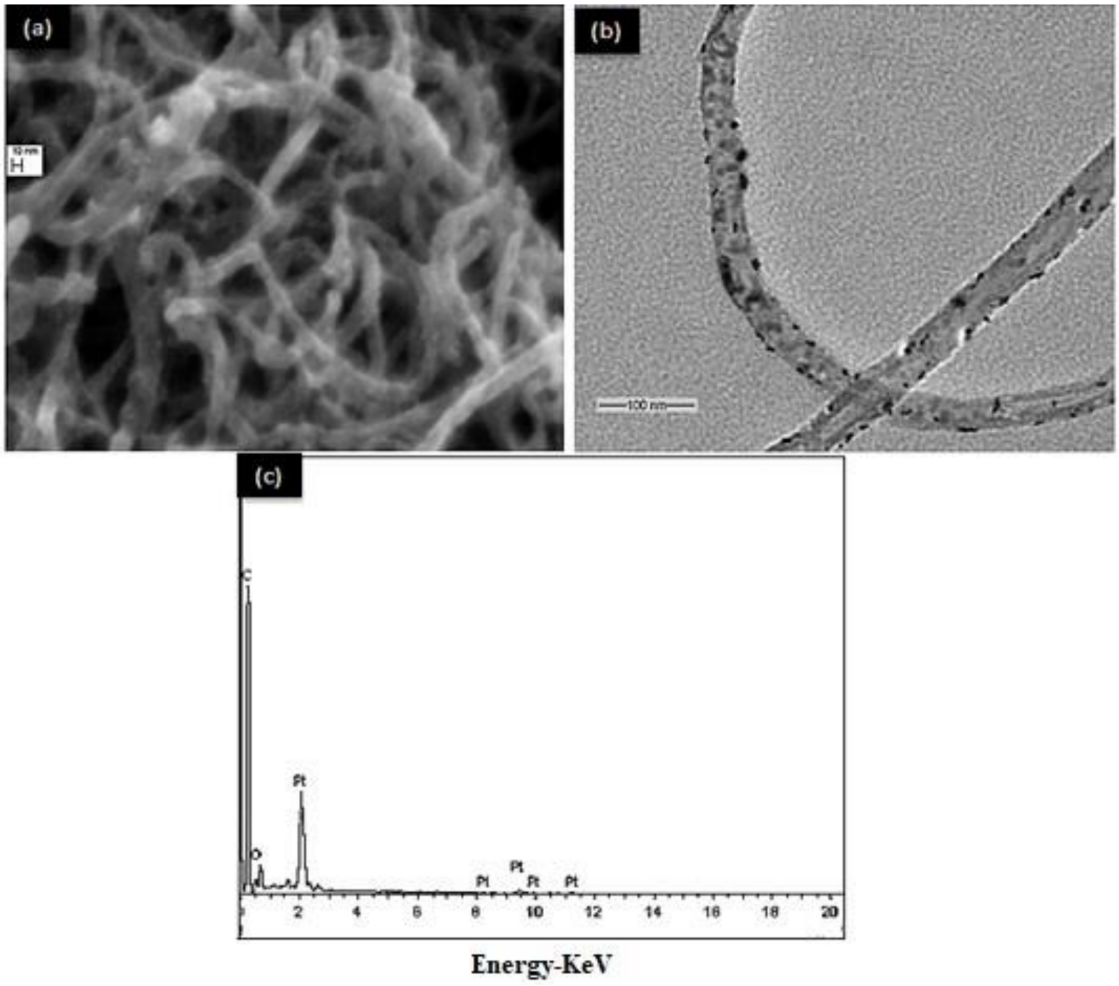

Figure 2. (**a**) FESEM, (**b**) TEM, and (**c**) EDX pattern of CNT/Pt nanocomposite.

3.2. Attachment of Microorganisms on the Anode Electrode

Figure 3 shows the morphology of the anode electrode and the attachment of microorganisms. It indicates clearly that various types of bacteria are attached to the electrode surface. They utilize the organic substrate of the feed, growing and producing electrons and protons which will be transferred to the cathode for electricity production [37].

Glucose was used as the substrate in the MFC. The reactions which occurred at the cathode and anode are summarized in Equations (4) and (5), respectively.

$$C_6H_{12}O_6 + 6H_2O \longrightarrow 6CO_2 + 24\,e^- + 24H^+ \quad (4)$$

$$O_2 + 24\,e^- + 24H^+ \longrightarrow 12H_2O \quad (5)$$

The oxidation of one mole of glucose in an anaerobic condition produces 24 mol electrons and protons. In our previous study.

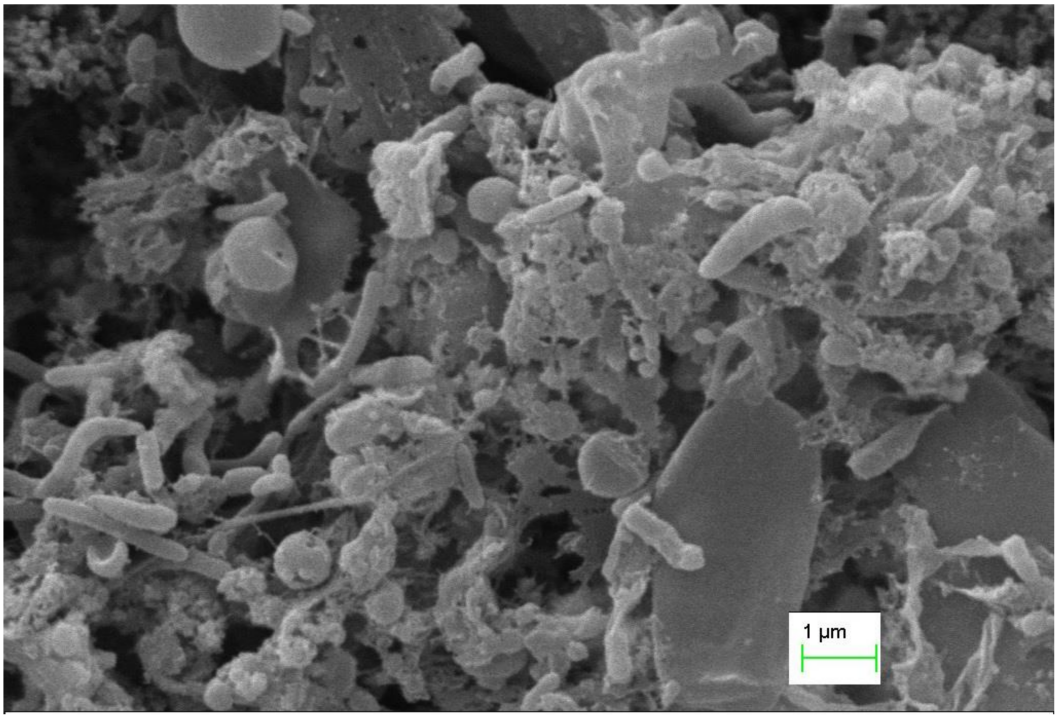

Figure 3. Attachment of microorganisms on the electrode.

3.3. Power Density

By changing the external load on the MFC, a power density graph can be drawn as shown in Figure 4.

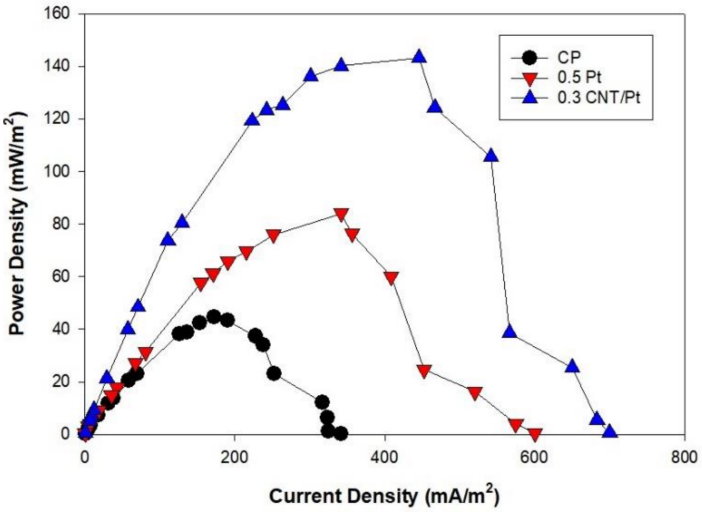

Figure 4. Power density graph of some electrodes.

The maximum power density of neat CP was 44.7 mW/m^2 at 172.66 mA/m^2. It increased by elevating the Pt amount and reached the maximum amount of 84.01 mW/m^2 (341 mA/m^2) for 0.5 mg/cm^2. However, for CNT/Pt cathode electrode, the power density augmented with rising the amount of CNT/Pt up to 0.3 mg/cm^2, in which the power density reached 143.1 mW/m^2 and remained almost constant [29].

Like previous studies [24,25], the nanocomposite cathode catalyst produced a higher power density than Pt.

The Pt nanoparticles placed on the CNT surface can absorb more hydrogen (H^+) ions due to the more open active surface, compared to Pt. The role of these particles in the

dissociation of the hydrogen molecule is critical and leads to an increase in the amount of adsorbed hydrogen by Van der Waals force [12]. In addition, the power was approximately constant without augmentation in CNT/Pt of over 0.3 mg/cm^2. The latter result shows that the diffusion resistance of the cathode raised because of a depletion in the oxygen diffusion rate that offsets the elevation of the catalyst [38].

3.4. Polarization Curve

The polarization curve of different systems is demonstrated in Figure 5. Typically, the voltage will decline by an increase in current density [39].

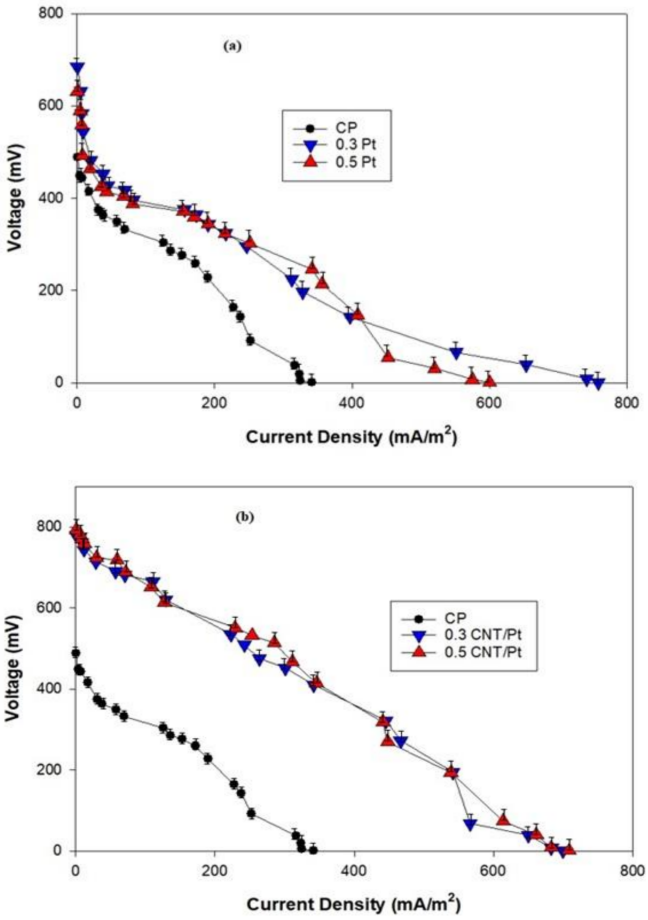

Figure 5. Effect of different kinds of electrodes on the polarization curve of fabricated MFC (**a**) Pt (**b**) CNT/Pt.

The internal resistance of the system was measured by the polarization curve and through mathematical calculations. Internal resistance is the slope of the voltage-current curve [40]. Therefore, a higher slope of the polarization curve means that the internal resistance is higher resulting in lower electricity production [41]. Table 1 indicates the internal resistance, maximum produced power, maximum current, and internal resistance at a maximum power density of different MFCs.

Table 1. Information taken from the MFCs.

Cathode Electrode	Internal Resistance (Ω)	P_{max} (mW/m^2)	I_{max} (mA/m^2) at P_{max}	OCV at SS Condition (mV)
CP	1084	44.7	172.7	493
0.1 Pt	894	53.4	159.5	587
0.2 Pt	873	77	327.1	687
0.3 Pt	812	73	246.7	693
0.4 Pt	811	75.9	251.6	673
0.5 Pt	810	84.1	341.7	672
0.1 CNT/Pt	587	73.5	221.3	746
0.2 CNT/Pt	593	125	288.7	787
0.3 CNT/Pt	551	143.1	445.8	794
0.4 CNT/Pt	564	146	312	811
0.5 CNT/Pt	573	146.8	285.6	815

Overall, the system that worked with CP as a cathode had the highest internal resistance of about 1084 Ω. The internal resistance decreased to 810 Ω by increasing the concentration of Pt to 0.5 mg/cm^2 as the lowest internal resistance among all Pt electrodes in this study. Moreover, in CNT/Pt nanocomposite, the lowest was 551 Ω for 0.3 mg/cm^2 CNT/Pt. This shows that the CNT/Pt composite had an internal resistance about 35% lower than Pt which may be attributed to the better electrical and catalytic activity, and especially higher conductivity, of the CNT/Pt nanocomposite electrode compared to Pt [42,43].

3.5. COD Removal and Coulombic Efficiency

Figure 6 demonstrates the COD removal, as well as the CE of the different systems.

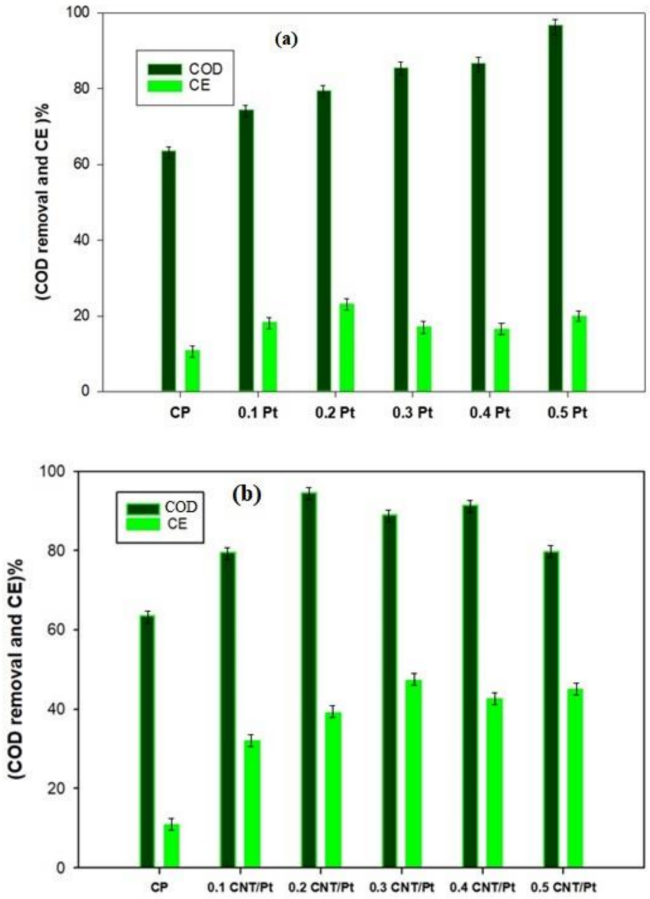

Figure 6. CE and COD removal of (**a**) Pt and (**b**) CNT/Pt electrodes.

As can be seen in Figure 6a, the highest and lowest CEs of 23% and 10.77% belonged to the CP coated by 0.2 mg/cm^2 Pt and neat CP, respectively. This means that more current is obtained from a substrate in the electrode by 0.2 mg/cm^2 Pt, in comparison with other Pt electrodes. Furthermore, the figure reveals that all electrodes coated by Pt had high COD removal of more than 70% indicating that MFCs are a proper method for COD removal [44,45]. Figure 6b shows the COD removal and CE of nanocomposite electrodes. The figure represents that the highest CE is related to the CP coated by 0.3 mg/cm^2 CNT/Pt around 47.159% in 88.9% COD removal. On the other hand, the lowest CE was 31.97% in 79.5% COD removal for 0.1 mg/cm^2 CNT/Pt. It should be noted that the COD removal for all nanocomposite electrode systems is >80%. For Pt electrodes, by increasing the concentration of Pt, COD removal and CE augment, while it did not exert the same impact on CNT/Pt. This can be observed in the internal resistance of the MFCs as well. For the Pt electrodes, by increasing the concentration of Pt, reduction occurs in internal resistance and then remains almost constant. However, it is not the same for CNT/Pt. In other words, elevation in internal resistance leads to a more complicated transfer of electrons from anode to cathode. Consequently, the power of the system for degrading organic substrates decreases resulting in diminished COD removal [46,47].

Table 2 compares the power density production and COD removal of different MFCs.

Table 2. Application of some cathode catalysts in MFC.

Cathode Catalyst	PEM	Power Density (mW/m^2)	COD Removal (%)	References
CoNiAl-LDH CoNiAl-LDH@$NiCo_2O_4$	Nafion N966	87.91 85.28	87.38 85.81	[48]
Pt-coated titanium	Ultrex CMI-7000)	271	-	[49]
SGO-TiO_2-PANi TiO_2-PANi Pt	Nafion 117	904.18 561.5 483.5	- - -	[50]
Pt CuZn C	Clayware based ceramic cylinder	110 75.1 19.2	90 87 77	[51]
Pt	Nafion 117 Nafion 117-SPVDF Laminated 117-SPVDF	481.55 446 413	93.97 90.27 84.15	[52]
Pt (PANi-Co-PPy)@TiO_2	Nafion 117	481 987	90.48 81.2	[22]
Pt CNT/Pt C	Nafion 117	84.1 143.1 44.7	96.8 88.9 63.5	This study

3.6. LSV Analysis

The activity of oxygen reduction on the cathode electrodes at diverse concentrations of Pt catalyst (Figure 7a) and CNT/Pt (Figure 7b) catalyst were compared together using LSV. Figure 6a indicates that the higher amount of Pt improved the ORR activity and the electrode with 0.5 mg/L Pt had the highest catalytic performance. On the other hand, for CNT/Pt, the catalytic performance augmented up to 0.3 mg/L CNT/Pt and then started to decline. This might be because the CNT weakens oxygen bonds resulting in lower activation energy. Moreover, the amount of generated current density by CNT/Pt electrodes is generally equal to or higher than the generated current by the Pt electrodes [19].

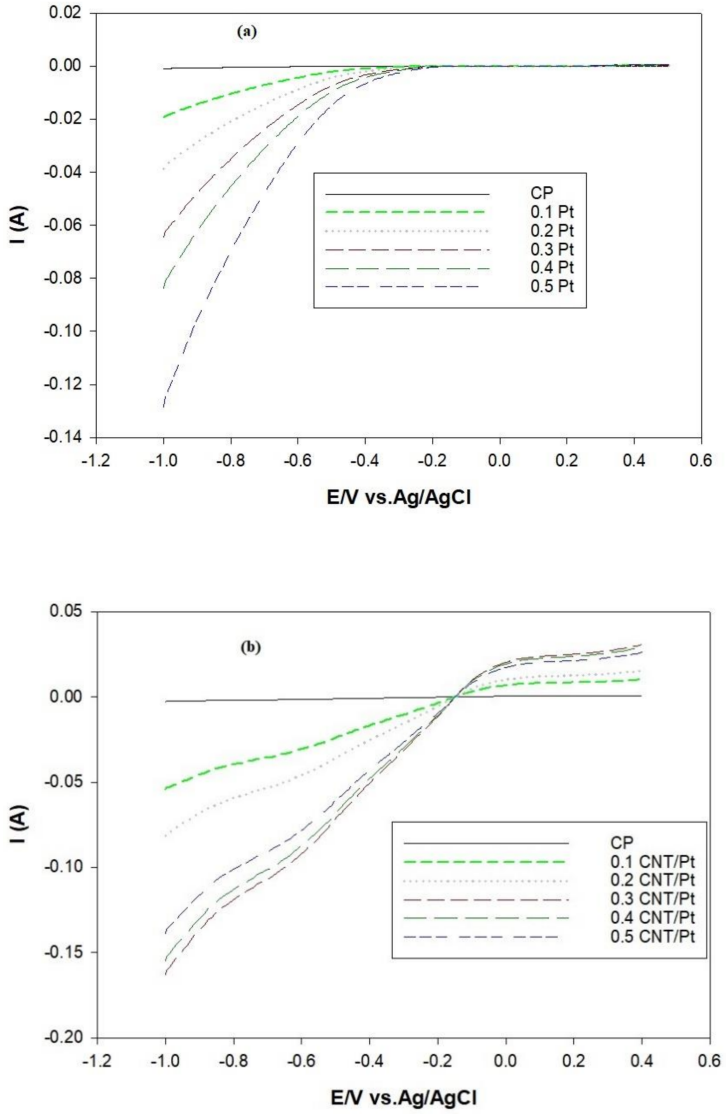

Figure 7. LSV patterns of (**a**) Pt and (**b**) CNT/Pt at different concentrations.

4. Conclusions

Sustainable energy production and wastewater treatment are some of the main parameters of industrial growth in the new era. MFC is a device that converts waste to energy. In this study, CNT/Pt nanocomposite in cathode catalysts was fabricated and applied as the cathode catalyst in MFC. It was made by drop-by-drop mixing of H_2PtCl_6 and CNT. Afterward, it was applied in the MFC for wastewater treatment and clean energy production. Our findings revealed that MFC showed better performance in terms of power generation and CE with the carbon nanocomposite cathode catalyst, compared to pure platinum.

The CNT provided more space for the attachment of Pt nanoparticles and facilitated the dissociation of protons and ORR by anticipating a higher surface area.

Furthermore, by decreasing the amount of Pt in the cathode, the capital cost of the MFC is reduced, making it more economical and applicable for societies and industries.

The nanocomposites diminished the activation energy and indicated great catalytic activity and therefore, can be a proper alternative for pure Pt. However, the optimization of the amount of nanocomposite should always be considered.

It was found that 0.3 mg/cm^2 CNT/Pt cathode catalyst produced 1.7 more power density compared to 0.5 mg/cm^2 Pt. It had also lower internal resistance (551 Ω), compared to the 0.5 mg/cm^2 Pt (810 Ω). Moreover, it had the highest CE (47.159%) and was shown to

be the most active catalyst. This research opened a new window towards sustainable clean energy production and environmental remediation.

Author Contributions: Methodology, Y.H.T.; formal analysis, M.S.; resources, M.G. All authors have read and agreed to the published version of the manuscript.

Funding: This research received no external funding.

Institutional Review Board Statement: Not applicable.

Informed Consent Statement: Not applicable.

Conflicts of Interest: The authors declare no conflict of interest.

References

1. Arulmani, S.R.B.; Gnanamuthu, H.L.; Kandasamy, S.; Govindarajan, G.; Alsehli, M.; Elfasakhany, A.; Pugazhendhi, A.; Zhang, H. Sustainable bioelectricity production from *Amaranthus viridis* and *Triticum aestivum* mediated plant microbial fuel cells with efficient electrogenic bacteria selections. *Process. Biochem.* **2021**, *107*, 27–37. [CrossRef]
2. Sedighi, M.; Mohammadi, M. CO_2 hydrogenation to light olefins over Cu-CeO_2/SAPO-34 catalysts: Product distribution and optimization. *J. CO_2 Util.* **2020**, *35*, 236–244. [CrossRef]
3. Sedighi, M.; Ghasemi, M.; Mohammadi, M.; Hassan, S.H.A. A novel application of a neuro–fuzzy computational technique in modeling of thermal cracking of heavy feedstock to light olefin. *RSC Adv.* **2014**, *4*, 28390–28399. [CrossRef]
4. Sallam, E.; Khairy, H.; Elnouby, M.; Fetouh, H. Sustainable electricity production from seawater using Spirulina platensis microbial fuel cell catalyzed by silver nanoparticles-activated carbon composite prepared by a new modified photolysis method. *Biomass Bioenergy* **2021**, *148*, 106038. [CrossRef]
5. Ghasemi, M.; Mohammadi, M.; Sedighi, M. Sustainable production of light olefins from greenhouse gas CO_2 over SAPO-34 supported modified cerium oxide. *Microporous Mesoporous Mater.* **2020**, *297*, 110029. [CrossRef]
6. Obileke, K.; Onyeaka, H.; Meyer, E.L.; Nwokolo, N. Microbial fuel cells, a renewable energy technology for bio-electricity generation: A mini-review. *Electrochem. Commun.* **2021**, *125*, 107003. [CrossRef]
7. Mohammadi, M.; Sedighi, M.; Natarajan, R.; Hassan, S.H.A.; Ghasemi, M. Microbial fuel cell for oilfield produced water treatment and reuse: Modelling and process optimization. *Korean J. Chem. Eng.* **2020**, *38*, 72–80. [CrossRef]
8. Shamshiri, A.; Alimohammadi, V.; Sedighi, M.; Jabbari, E.; Mohammadi, M. Enhanced removal of phosphate and nitrate from aqueous solution using novel modified natural clinoptilolite nanoparticles: Process optimization and assessment. *Int. J. Environ. Anal. Chem.* **2020**, 1–20. [CrossRef]
9. Mohammadi, M.; Sedighi, M.; Ghasemi, M. Systematic investigation of simultaneous removal of phosphate/nitrate from water using Ag/rGO nanocomposite: Development, characterization, performance and mechanism. *Res. Chem. Intermed.* **2021**, *47*, 1377–1395. [CrossRef]
10. Sedighi, M.; Mohammadi, M. Application of green novel NiO/ZSM-5 for removal of lead and mercury ions from aqueous solution: Investigation of adsorption parameters. *J. Water Environ. Nanotechnol.* **2018**, *3*, 301–310. [CrossRef]
11. Shahveh, S.; Sedighi, M.; Mohammadi, M. A Novel Application of Combined Biological and Physical Method for Nitrate and Nitrite Removal from Water. *J. Environ. Sci. Technol.* **2020**, *22*, 183–192. [CrossRef]
12. Lin, C.-W.; Lai, C.-Y.; Liu, S.-H.; Chen, Y.-R.; Alfanti, L.K. Enhancing bioelectricity generation and removal of copper in microbial fuel cells with a laccase-catalyzed biocathode. *J. Clean. Prod.* **2021**, *298*, 126726. [CrossRef]
13. Ghasemi, M.; Ahmad, A.; Jafary, T.; Azad, A.K.; Kakooei, S.; Daud, W.R.W.; Sedighi, M. Assessment of immobilized cell reactor and microbial fuel cell for simultaneous cheese whey treatment and lactic acid/electricity production. *Int. J. Hydrogen Energy* **2017**, *42*, 9107–9115. [CrossRef]
14. Hisham, S.; Khan, F.A.; Aljlil, S.A.; Ghasemi, M. Investigating new techniques for the treatment of oil field produced water and energy production. *SN Appl. Sci.* **2019**, *1*, 646. [CrossRef]
15. Ghasemi, M.; Daud, W.R.W.; Alam, J.; Ilbeygi, H.; Sedighi, M.; Ismail, A.F.; Yazdi, M.H.; Aljlil, S.A. Treatment of two different water resources in desalination and microbial fuel cell processes by poly sulfone/Sulfonated poly ether ether ketone hybrid membrane. *Energy* **2016**, *96*, 303–313. [CrossRef]
16. Yu, B.; Tian, J.; Feng, L. Remediation of PAH polluted soils using a soil microbial fuel cell: Influence of electrode interval and role of microbial community. *J. Hazard. Mater.* **2017**, *336*, 110–118. [CrossRef]
17. Ghasemi, M.; Daud, W.R.W.; Ismail, M.; Rahimnejad, M.; Ismail, A.F.; Leong, J.X.; Miskan, M.; Ben Liew, K. Effect of pre-treatment and biofouling of proton exchange membrane on microbial fuel cell performance. *Int. J. Hydrogen Energy* **2013**, *38*, 5480–5484. [CrossRef]
18. Ghasemi, M.; Shahgaldi, S.; Ismail, M.; Kim, B.H.; Yaakob, Z.; Daud, W.R.W. Activated carbon nanofibers as an alternative cathode catalyst to platinum in a two-chamber microbial fuel cell. *Int. J. Hydrogen Energy* **2011**, *36*, 13746–13752. [CrossRef]
19. Ghasemi, M.; Daud, W.R.W.; Hassan, S.H.; Oh, S.-E.; Ismail, M.; Rahimnejad, M.; Jahim, J.M. Nano-structured carbon as electrode material in microbial fuel cells: A comprehensive review. *J. Alloys Compd.* **2013**, *580*, 245–255. [CrossRef]

20. Zhang, Q.; Liu, L. A microbial fuel cell system with manganese dioxide/titanium dioxide/graphitic carbon nitride coated granular activated carbon cathode successfully treated organic acids industrial wastewater with residual nitric acid. *Bioresour. Technol.* **2020**, *304*, 122992. [CrossRef]
21. Ali, J.; Wang, L.; Waseem, H.; Djellabi, R.; Oladoja, N.; Pan, G. FeS@rGO nanocomposites as electrocatalysts for enhanced chromium removal and clean energy generation by microbial fuel cell. *Chem. Eng. J.* **2020**, *384*, 123335. [CrossRef]
22. Pattanayak, P.; Papiya, F.; Kumar, V.; Singh, A.; Kundu, P.P.; Pattanayak, P.; Papiya, F.; Kumar, V.; Singh, A.; Kundu, P.P. Performance evaluation of poly(aniline-co-pyrrole) wrapped titanium dioxide nanocomposite as an air-cathode catalyst material for microbial fuel cell. *Mater. Sci. Eng. C* **2021**, *118*, 111492. [CrossRef] [PubMed]
23. Türk, K.; Kruusenberg, I.; Kibena-Põldsepp, E.; Bhowmick, G.D.; Kook, M.; Tammeveski, K.; Matisen, L.; Merisalu, M.; Sammelselg, V.; Ghangrekar, M.; et al. Novel multi walled carbon nanotube based nitrogen impregnated Co and Fe cathode catalysts for improved microbial fuel cell performance. *Int. J. Hydrogen Energy* **2018**, *43*, 23027–23035. [CrossRef]
24. Ghasemi, M.; Nassef, A.M.; Al-Dhaifallah, M.; Rezk, H. Performance improvement of microbial fuel cell through artificial intelligence. *Int. J. Energy Res.* **2020**, *45*, 342–354. [CrossRef]
25. Du, Y.; Ma, F.-X.; Xu, C.-Y.; Yu, J.; Li, D.; Feng, Y.; Zhen, L. Nitrogen-doped carbon nanotubes/reduced graphene oxide nanosheet hybrids towards enhanced cathodic oxygen reduction and power generation of microbial fuel cells. *Nano Energy* **2019**, *61*, 533–539. [CrossRef]
26. Wang, Y.; Zhong, K.; Li, H.; Dai, Y.; Zhang, H.; Zuo, J.; Yan, J.; Xiao, T.; Liu, X.; Lu, Y.; et al. Bimetallic hybrids modified with carbon nanotubes as cathode catalysts for microbial fuel cell: Effective oxygen reduction catalysis and inhibition of biofilm formation. *J. Power Sources* **2021**, *485*, 229273. [CrossRef]
27. Majidi, M.R.; Farahani, F.S.; Hosseini, M.G.; Ahadzadeh, I. Low-cost nanowired α-MnO_2/C as an ORR catalyst in air-cathode microbial fuel cell. *Bioelectrochemistry* **2019**, *125*, 38–45. [CrossRef]
28. Babanova, S.; Santoro, C.; Jones, J.; Phan, T.; Serov, A.; Atanassov, P.; Bretschger, O.; Babanova, S.; Santoro, C.; Jones, J.; et al. Practical demonstration of applicability and efficiency of platinum group metal-free based catalysts in microbial fuel cells for wastewater treatment. *J. Power Sources* **2021**, *491*, 229582. [CrossRef]
29. Ghasemi, M.; Halakoo, E.; Sedighi, M.; Alam, J.; Sadeqzadeh, M.; Ghasemi, M.; Halakoo, E.; Sedighi, M.; Alam, J.; Sadeqzadeh, M. Performance Comparison of Three Common Proton Exchange Membranes for Sustainable Bioenergy Production in Microbial Fuel Cell. *Procedia CIRP* **2015**, *26*, 162–166. [CrossRef]
30. Khan, F.A.; Hisham, S.; Ghasemi, M. Oil field produced water recovery and boosting the quality for using in membrane less fuel cell. *SN Appl. Sci.* **2019**, *1*, 510. [CrossRef]
31. Jafary, T.; Aljlil, S.A.; Alam, J.; Ghasemi, M. Effect of the Membrane Type and Resistance Load on the Performance of the Microbial Fuel Cell: A Step ahead of Microbial Desalination Cell Establishment. *J. Jpn. Inst. Energy* **2017**, *96*, 346–351. [CrossRef]
32. Shamshirgaran, S.; Al-Kayiem, H.; Sharma, K.; Ghasemi, M. State of the Art of Techno-Economics of Nanofluid-Laden Flat-Plate Solar Collectors for Sustainable Accomplishment. *Sustainability* **2020**, *12*, 9119. [CrossRef]
33. Sedighi, M.; Aljlil, S.A.; Alsubei, M.D.; Ghasemi, M.; Mohammadi, M. Performance optimisation of microbial fuel cell for wastewater treatment and sustainable clean energy generation using response surface methodology. *Alex. Eng. J.* **2018**, *57*, 4243–4253. [CrossRef]
34. Ghasemi, M.; Daud, W.R.W.; Rahimnejad, M.; Rezayi, M.; Fatemi, A.; Jafari, Y.; Somalu, M.R.; Manzour, A. Copper-phthalocyanine and nickel nanoparticles as novel cathode catalysts in microbial fuel cells. *Int. J. Hydrogen Energy* **2013**, *38*, 9533–9540. [CrossRef]
35. Bharti, A.; Cheruvally, G.; Muliankeezhu, S. Microwave assisted, facile synthesis of Pt/CNT catalyst for proton exchange membrane fuel cell application. *Int. J. Hydrogen Energy* **2017**, *42*, 11622–11631. [CrossRef]
36. Zhao, N.; Ma, Z.; Song, H.; Xie, Y.; Zhang, M. Enhancement of bioelectricity generation by synergistic modification of vertical carbon nanotubes/polypyrrole for the carbon fibers anode in microbial fuel cell. *Electrochim. Acta* **2019**, *296*, 69–74. [CrossRef]
37. Ben Liew, K.; Daud, W.R.W.; Ghasemi, M.; Leong, J.X.; Lim, S.S.; Ismail, M. Non-Pt catalyst as oxygen reduction reaction in microbial fuel cells: A review. *Int. J. Hydrogen Energy* **2014**, *39*, 4870–4883. [CrossRef]
38. Wang, X.; Yuan, C.; Shao, C.; Zhuang, S.; Ye, J.; Li, B. Enhancing oxygen reduction reaction by using metal-free nitrogen-doped carbon black as cathode catalysts in microbial fuel cells treating wastewater. *Environ. Res.* **2020**, *182*, 109011. [CrossRef]
39. Negassa, L.W.; Mohiuddin, M.; Tiruye, G.A. Treatment of brewery industrial wastewater and generation of sustainable bio-electricity by microbial fuel cell inoculated with locally isolated microorganisms. *J. Water Process. Eng.* **2021**, *41*, 102018. [CrossRef]
40. Elshobary, M.E.; Zabed, H.M.; Yun, J.; Zhang, G.; Qi, X.; Elshobary, M.E.; Zabed, H.M.; Yun, J.; Zhang, G.; Qi, X. Recent insights into microalgae-assisted microbial fuel cells for generating sustainable bioelectricity. *Int. J. Hydrogen Energy* **2021**, *46*, 3135–3159. [CrossRef]
41. Rossi, R.; Logan, B.E. Unraveling the contributions of internal resistance components in two-chamber microbial fuel cells using the electrode potential slope analysis. *Electrochim. Acta* **2020**, *348*, 136291. [CrossRef]
42. Rahimnejad, M.; Ghasemi, M.; Najafpour, G.; Ismail, M.; Mohammad, A.W.; Ghoreyshi, A.; Hassan, S.H. Synthesis, characterization and application studies of self-made Fe_3O_4/PES nanocomposite membranes in microbial fuel cell. *Electrochim. Acta* **2012**, *85*, 700–706. [CrossRef]
43. Parkhey, P.; Sahu, R. Microfluidic microbial fuel cells: Recent advancements and future prospects. *Int. J. Hydrogen Energy* **2021**, *46*, 3105–3123. [CrossRef]

44. Xin, S.; Shen, J.; Liu, G.; Chen, Q.; Xiao, Z.; Zhang, G.; Xin, Y. Electricity generation and microbial community of single-chamber microbial fuel cells in response to Cu_2O nanoparticles/reduced graphene oxide as cathode catalyst. *Chem. Eng. J.* **2020**, *380*, 122446. [CrossRef]
45. Ullah, Z.; Zeshan, S. Effect of substrate type and concentration on the performance of a double chamber microbial fuel cell. *Water Sci. Technol.* **2020**, *81*, 1336–1344. [CrossRef]
46. Li, S.; Ho, S.-H.; Hua, T.; Zhou, Q.; Li, F.; Tang, J. Sustainable biochar as electrocatalysts for the oxygen reduction reaction in microbial fuel cells. *Green Energy Environ.* **2020**. [CrossRef]
47. Gadkari, S.; Gu, S.; Sadhukhan, J. Two-dimensional mathematical model of an air-cathode microbial fuel cell with graphite fiber brush anode. *J. Power Sources* **2019**, *441*, 227145. [CrossRef]
48. Khajeh, R.T.; Aber, S.; Zarei, M. Comparison of $NiCo_2O_4$, CoNiAl-LDH, and CoNiAl-LDH@$NiCo_2O_4$ performances as ORR catalysts in MFC cathode. *Renew. Energy* **2020**, *154*, 1263–1271. [CrossRef]
49. Taskan, E.; Hasar, H.; Taskan, E.; Hasar, H. Comprehensive Comparison of a New Tin-Coated Copper Mesh and a Graphite Plate Electrode as an Anode Material in Microbial Fuel Cell. *Appl. Biochem. Biotechnol.* **2015**, *175*, 2300–2308. [CrossRef]
50. Papiya, F.; Pattanayak, P.; Kumar, V.; Das, S.; Kundu, P.P.; Papiya, F.; Pattanayak, P.; Kumar, V.; Das, S.; Kundu, P.P. Sulfonated graphene oxide and titanium dioxide coated with nanostructured polyaniline nanocomposites as an efficient cathode catalyst in microbial fuel cells. *Mater. Sci. Eng. C* **2020**, *108*, 110498. [CrossRef]
51. Das, I.; Das, S.; Ghangrekar, M. Application of bimetallic low-cost CuZn as oxygen reduction cathode catalyst in lab-scale and field-scale microbial fuel cell. *Chem. Phys. Lett.* **2020**, *751*, 137536. [CrossRef]
52. Kumar, V.; Kumar, P.; Nandy, A.; Kundu, P. Fabrication of laminated and coated Nafion 117 membranes for reduced mass transfer in microbial fuel cells. *RSC Adv.* **2016**, *6*, 21526–21534. [CrossRef]